

## THE R-PROCESS IN THE EARLY GALAXY

JENNIFER A. JOHNSON

OCIW, 813 Santa Barbara St., Pasadena, CA 91101

AND

MICHAEL BOLTE

UCO/Lick Observatory, University of California, Santa Cruz, CA 95064

*To be published in ApJ*

### ABSTRACT

We report Sr, Pd and Ag abundances for a sample of metal-poor field giants and analyze a larger sample of Y, Zr, and Ba abundances. The [Y/Zr] and [Pd/Ag] abundance ratios are similar to those measured for the r-process-rich stars CS 22892-052 and CS 31082-001. The [Pd/Ag] ratio is larger than predicted from the solar-system r-process abundances. The constant [Y/Zr] and [Sr/Y] values in the field stars places strong limits on the contributions of the weak s-process and the main s-process to the light neutron-capture elements. Stars in the globular cluster M 15 possess lower [Y/Zr] values than the field stars. There is a large dispersion in [Y/Ba]. Because the r-process is responsible for the production of the heavy elements in the early Galaxy, these dispersions require varying light-to-heavy ratios in r-process yields.

*Subject headings:* nuclear reactions, nucleosynthesis, abundances—stars: abundances—Galaxy: halo

### 1. INTRODUCTION

Burbidge et al. (1957) and Cameron (1957) showed that only two sets of physical conditions were necessary to explain the abundances of the heavy ( $A > 65$ ) elements in the solar system. Because of strong Coulomb forces, the build-up of heavier nuclei happens through neutron-capture. The first of these neutron-capture processes is the s-process, where neutron captures onto seed nuclei take place much more slowly than  $\beta$ -decays. The s-process is thought to take place in two distinct environments. The ‘main’ s-process occurs in low-mass AGB stars, while the ‘weak’ s-process occurs during helium burning in massive stars. While the main s-process can make neutron-rich material up to  $^{209}\text{Bi}$  (Clayton & Rassbach 1967), the weak s-process is not predicted to make significant amounts of material with  $A > 90$  (Couch, Schmiedekamp, & Arnett 1974). The second neutron-capture process, the r-process, takes place when conditions are such that neutron capture rates are much higher than  $\beta$ -decay rates. It produces a distinctive pattern in the abundance ratios, the most noticeable features being the so-called r-process peaks. These peaks, at  $A \sim 80$ , 130, and 196, are the signatures of nucleosynthesis events which reached the neutron magic numbers of 50, 82, and 126.

Despite having been identified as taking place in an environment with rapid neutron captures, the astrophysical phenomena that create the r-process remain unidentified. The neutrino wind in Type II SN showed promise (Woosley & Hoffman 1992; Woosley et al. 1994), but two problems arose. First, there remain questions about whether the entropy in the wind is sufficiently high to produce the r-process (Takahashi, Witti, & Janka 1994; Qian & Woosley 1996, but see Otsuki et al. 2000; Wanajo et al. 2001). Also, Freiburghaus et al. (1999a) found that high-entropy wind models cannot produce an r-process pattern for  $A < 110$  because those elements are synthesized during the low-entropy, neutron-deficient  $\alpha$ -rich freezeout

phase of the wind. Witti, Janka, & Takahashi (1994) and Woosley et al. (1994) also show that the elements near  $N=50$  are overproduced relative to the more massive nuclei in neutrino wind models. So either the neutrino-wind is not the source of any r-process products, or the conditions are such that the material with  $A < 110$  is either not ejected or is diluted. Models have shown that merging neutron stars may be the source of significant amounts of r-process material (e.g. Lattimer & Schramm 1974; Rosswog et al. 2000). Freiburghaus, Rosswog & Thielemann (1999b) did parameterized calculations of the nucleosynthesis in the ejecta and found that it could be a source for nuclei with  $A \gtrsim 130$ . An earlier suggestion that the r-process occurred in helium-burning regions, either cores of low-mass stars or in the helium shell in SN, was rejected because unacceptably large amounts of  $^{13}\text{C}$  were required to make the  $A \sim 195$  peak (Cowan, Cameron & Truran 1985). However, helium-burning phases can still make r-process isotopes in the range  $A \sim 80$  with about half as much  $^{13}\text{C}$ . Truran, Cowan, & Fields (2001) updated the calculations for the helium-shell shock r-process and find that for normal amounts of C, it can provide interesting amounts of material with  $A < 130$ .

Abundances in metal-poor stars provide insight into the r-process because they bear the marks of relatively few nucleosynthesis events and because the r-process is thought to be the sole source of many of the heavy elements in the early Galaxy (Truran 1981). However, alternative sources, such as the weak s-process, may contribute substantial amounts to the lightest of the neutron-capture elements, such as Sr, Y and Zr (e.g. Prantzos, Hashimoto & Nomoto 1990). In recent years, much new information has become available on the abundances of heavy elements in metal-poor stars (e.g. Gilroy et al. 1988; McWilliam et al. 1995; Ryan et al. 1996; Westin et al. 2000; Burris et al. 2000), revealing a wide diversity in some abundance ratios, such as [Sr/Ba] and a remarkable consistency in others, such as [Ba/Eu]. The information on the intermediate-mass ele-

ments such as Pd and Ag is particularly interesting, since the abundance ratios in one star, CS 22892-052, showed a larger difference between the abundances of the odd-Z and even-Z elements than seen in the solar system (Sneden et al. 2000a).

Johnson (2002) (Paper I) presented the abundances of up to 17 neutron-capture elements in a sample of 22 metal-poor ( $[\text{Fe}/\text{H}] < -1.7$ ) field red giants. In this paper we add Sr abundances for these stars, as well as Pd and Ag abundances for three stars from this sample. We then analyze the abundance patterns for all the heavy elements in the Paper I sample to learn more about the r-process in the early Galaxy.

## 2. OBSERVATIONS AND DATA REDUCTION

The full details of the observations and data reduction are in Paper I. Briefly, we obtained high-resolution spectra on two echelle spectrographs. We observed 12 stars with HIRES (Vogt et al. 1994) on Keck I in May and June 1997. These data cover from 3200Å to 4700Å with  $R \sim 45,000$ . The S/N was  $\sim 200$  at 4000Å. We also observed 21 stars, including 11 of the 12 HIRES stars, with the Hamilton on the Shane 3-meter at Lick Observatory (Vogt 1987). The Hamilton data have larger wavelength coverage (3800Å to 7000Å) and higher resolution ( $R \sim 60,000$ ), but lower S/N ( $\sim 100$  at 6000Å). We measured over 7000 equivalent widths (EWs) and synthesized over 200 additional lines. Paper I reports the abundances of 30 elements for our sample of stars, including 17 neutron-capture elements.

We used Kurucz model atmospheres<sup>1</sup>. The effective temperature was chosen so that the abundance derived from Fe I lines did not depend on their excitation potential. Gravity was set from the ionization balance from the Fe I/Fe II lines. The microturbulent velocity ( $\xi$ ) was changed until there was no slope in the abundances vs. EW plot for the Fe I lines. The errors shown in this paper caused by uncertainties in the atmospheric parameters take into consideration random errors of  $\pm 100\text{K}$  in  $T_{\text{eff}}$ ,  $\pm 0.3$  dex in  $\log g$ , and  $\pm 0.3$  km/s in  $\xi$  as well as the scatter caused by inaccurate gf-values and EWs. Errors for abundance ratios consider the similarity of the two elements' response to atmospheric model parameter changes in the manner discussed in McWilliam et al. (1995) (Paper I). We note that when solar values are used, we used the meteoritic values from Anders & Grevesse (1989).

However, three interesting elements were not considered in that study, Pd, Ag and Sr. Below we derive abundances for these three elements to bring to 20 the number of neutron-capture elements with measurements in our metal-poor star sample.

## 3. ABUNDANCES

### 3.1. *Pd and Ag*

We could only use one Pd and one Ag line to measure abundances. Both lines lie to the blue of 3500 Å where the spectrum, even in metal-poor stars, is very crowded. Therefore, we synthesized the spectrum in these regions. Examples for the Pd and Ag lines are shown in Figure 1. The initial line list was taken from Kurucz CD-ROM 23 (Kurucz & Bell 1995) and modified when more recent

gf-values could be found. We also eliminated lines from the list that had no noticeable contribution to the spectral synthesis. For the Pd I line list, we used the gf-values of O'Brian et al. (1991) for the Fe I lines at 3404.290Å and 3404.360Å. The Co I line at 3405.13Å had hyperfine splitting (HFS) constants from Pickering (1996). The Pd line has a gf-value from Biémont et al. (1982). This region of the spectrum is also littered with NH lines. The gf-values and wavelengths for the NH lines were taken from Kurucz<sup>2</sup> and most have theoretically predicted wavelengths and gf-values. Luckily, none of the lines near Pd 3404Å were strong enough to show any absorption, mostly because they were  $^{15}\text{NH}$  lines. In support a lack of contamination we note that in their analysis of the solar spectrum, Biémont et al. (1982) found that using the EW of the 3404Å Pd line resulted in a  $\log \epsilon$  of 1.67 dex, very close to the average photospheric value of 1.69 dex and the meteoritic value of 1.70 dex (Anders & Grevesse 1989). In addition, several of our stars (e.g. Fig 2) show very little absorption in that region, indicating the lack of contaminants. Table 1 has our final line list. The problem with blending is more severe for the Ag line at 3280Å, since Kurucz lists some NH lines very close to the wavelength of the Ag line. We have set the NH strength in this region empirically. Synthesis of the solar spectrum with the Kurucz line lists revealed that the log gf-values for the 3280Å region should be increased by 0.4 dex relative to the log gf-values for the 3360Å NH region. In practice, we found an NH abundance using the 3360Å region for our halo stars, and then increased the N abundance to 0.4 dex when synthesizing the 3280Å region. The linelist in Table 2 contains the original Kurucz values. We note that if we did not adjust the NH absorption, the Ag values for HD 108577 and HD 186478 would be  $\sim 0.1 - 0.15$  dex higher, still in disagreement with the solar values. The stronger

<sup>2</sup><http://cfaku5.harvard.edu>

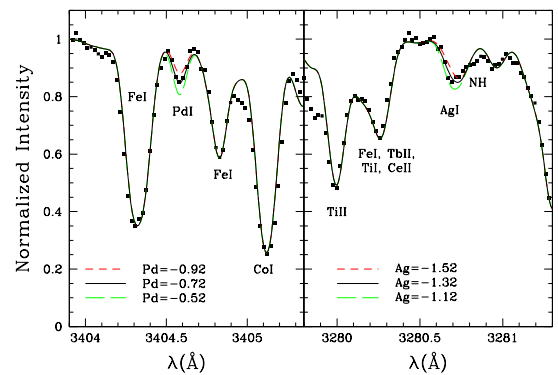


FIG. 1.— Synthesis of the 3404Å Pd I line and the 3280Å Ag I line in HD 186478 ( $[\text{Fe}/\text{H}] = -2.60$ ). The black solid line shows the best synthesis, while the other lines show changes of  $\pm 0.2$  dex. For the Pd synthesis, the Fe abundance has been increased 0.2 dex, the Co abundance decreased by  $-0.6$  dex and the Zr abundance increased by 0.3 dex over the abundances derived in Paper I. For the Ag synthesis, the Zr abundance ( $-0.2$  dex) has been decreased. We also adopted  $[\text{O}/\text{Fe}] = 1.00$  dex. These changes are not unexpected given the uncertainties in abundances and gf-values, but they had no effect on the derived Pd and Ag abundances.

<sup>1</sup>[http://cfaku5.harvard.edu/](http://cfaku5.harvard.edu)

TABLE 1  
LINELIST NEAR AG I AT 3280 Å

$\lambda$ Å	Species	E.P. eV	$\log gf$	$\lambda$ Å	Species	E.P. eV	$\log gf$
3279.010	CoI	3.13	-2.40	3280.957	NH	1.61	-1.61
3279.130	OH	1.50	-1.51	3280.957	NH	1.71	-1.08
3279.251	CoI	1.96	-0.85	3280.957	NH	1.71	-1.10
3279.255	OH	1.64	-1.85	3281.001	NH	1.82	-1.05
3279.266	ZrII	0.09	-0.23	3281.044	NH	2.16	-1.63
3279.325	ErII	0.64	-0.13	3281.101	CeII	0.88	-0.58
3279.733	FeI	2.99	-1.83	3281.125	VII	2.56	-0.63
3279.812	CuI	1.64	-2.17	3281.141	NH	1.82	-0.57
3279.839	CeII	0.29	-0.50	3281.196	NH	1.51	-0.59
3279.848	VII	2.37	0.01	3281.212	NH	1.82	-0.58
3279.972	HfII	0.45	-1.14	3281.304	FeII	1.04	-2.99
3279.995	TiII	1.12	-0.84	3281.328	NH	1.51	-0.61
3280.003	UII	0.11	-1.19	3281.328	NH	1.51	-0.62
3280.093	DyII	0.10	-0.53	3281.483	NdII	1.60	0.07
3280.155	OH	1.64	-2.25	3281.600	CoI	0.17	-3.76
3280.217	ErII	0.05	-0.67	3282.247	CoI	1.78	-2.84
3280.267	FeI	3.30	-0.22	3282.310	GdII	1.34	0.26
3280.312	TbII	0.00	0.13	3282.334	TiII	1.22	-0.29
3280.368	TiI	1.07	-2.25	3282.447	FeI	2.50	-2.00
3280.481	CeII	0.55	-0.07	3282.480	UII	0.00	-1.31
3280.536	RhI	0.19	-0.52	3282.540	VII	2.37	0.02
3280.577	RhI	0.43	-0.87	3282.689	NiI	0.17	-2.17
3280.677	AgI	0.00	-0.48	3282.705	OH	1.98	-1.39
3280.678	AgI	0.00	-0.46	3282.717	FeI	2.95	-2.08
3280.683	AgI	0.00	-0.94	3282.730	ZrI	0.15	-0.53
3280.685	AgI	0.00	-0.96	3282.766	NdII	0.00	-1.36
3280.735	ZrII	0.71	-1.10	3282.771	NH	1.32	-0.62
3280.759	NH	1.71	-0.57	3282.837	ZrII	1.83	0.30
3280.775	MnI	2.14	-2.23	3282.858	NH	1.32	-0.64
3280.775	FeI	3.02	-2.53	3282.858	NH	1.32	-0.66
3280.844	SmII	0.10	-1.09	3282.892	DyII	0.59	-1.00
3280.957	NH	1.61	-1.58	3282.904	FeI	3.27	-0.61
3280.957	NH	1.61	-1.60				

TABLE 2  
LINELIST NEAR PD I AT 3404 Å

$\lambda$ Å	Species	E.P. eV	$\log gf$	$\lambda$ Å	Species	E.P. eV	$\log gf$
3402.396	CrI	3.10	-0.56	3405.096	CoI	0.43	-1.56
3402.424	TiII	1.22	-1.00	3405.104	CoI	0.43	-0.88
3402.429	FeI	2.73	-1.84	3405.112	CoI	0.43	-1.48
3402.462	SmII	0.38	-0.56	3405.113	CoI	0.43	-1.77
3402.508	OsI	0.00	-2.25	3405.119	CoI	0.43	-0.99
3402.634	FeI	2.76	-2.14	3405.125	CoI	0.43	-1.47
3402.900	ZrII	1.53	-0.33	3405.127	CoI	0.43	-1.56
3403.084	SmII	0.49	-0.91	3405.131	CoI	0.43	-1.15
3403.271	FeI	2.83	-1.93	3405.136	CoI	0.43	-1.51
3403.344	TiI	1.07	-0.51	3405.138	CoI	0.43	-1.48
3403.345	CrII	2.43	-0.54	3405.141	CoI	0.43	-1.32
3403.346	MoI	1.42	-1.61	3405.145	CoI	0.43	-1.62
3403.597	CeII	0.52	-0.79	3405.147	CoI	0.43	-1.47
3403.693	ZrII	1.00	-0.60	3405.149	CoI	0.43	-1.49
3404.290	FeI	1.01	-2.58	3405.152	CoI	0.43	-1.84
3404.290	FeI	2.73	-0.67	3405.154	CoI	0.43	-1.51
3404.360	FeI	2.20	-0.88	3405.155	CoI	0.43	-1.63
3404.580	PdI	0.81	0.32	3405.159	CoI	0.43	-1.62
3404.764	FeI	2.73	-2.20	3405.159	CoI	0.43	-1.64
3404.830	ZrII	0.36	-0.70	3405.161	CoI	0.43	-1.84
3404.902	FeI	2.69	-2.60	3405.654	DyII	0.59	-0.66
3404.908	CeII	0.23	-0.65	3405.838	FeI	2.69	-1.86
3404.961	TiII	1.22	-2.72	3405.978	CeII	0.55	0.04
3405.064	TiI	1.05	-0.80	3406.437	FeI	3.27	-0.88
3405.079	CoI	0.43	-2.77	3406.552	FeI	2.45	-1.90
3405.087	CoI	0.43	-0.71	3406.800	FeI	2.22	-1.10

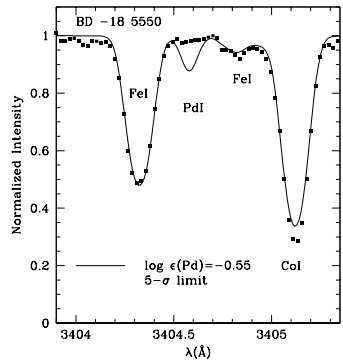


FIG. 2.— Synthesis of the 3404 Å Pd I line region in BD -18 5550 ( $[\text{Fe}/\text{H}] = -3.04$ ). The solid black line shows the  $5\sigma$  upper limit on the Pd abundance.

Ag line in BD +8 2548 makes it fairly immune to changes in the NH line strength. Ross & Aller (1972) and Crawford et al. (1998) found that the Ag line at 3280 in the Sun gives a  $\log \epsilon$  of 1.05 dex, below the meteoritic value of 1.24 dex (Anders & Grevesse 1989). The source of the discrepancy between the meteoritic and the photospheric values is unclear. Crawford et al. (1998) point out that an increase in the opacity by  $\sim 1.3$  in the Sun could solve the problem. Whether missing opacity on the same scale is present in our sample of metal-poor giant is not known. We note that the gf-value is a recent laboratory measurement (Fuhr & Wiese 1996) and is estimated to have a 10% uncertainty. Although HFS should not be a issue with a line this weak, we have nonetheless used the wavelengths and relative strengths from Ross & Aller (1972) to split the Fuhr & Wiese gf-value into HFS components. We estimate that our signal-to-noise in these regions as well as inaccuracies in our linelists limit our precision for both Pd I and Ag I to 0.2 dex. The inclusion of errors caused by our choices of model atmosphere parameters leads to a final error estimate of 0.25 dex. Our Pd and Ag abundances are listed in Table 2. In Table 2, we also list the  $5\sigma$  upper limits on the abundance of Pd for the stars with HIRES data. These limits were derived by generating synthetic spectra with different Pd abundances and then testing the goodness-of-fit to the HIRES data with a  $\chi^2$  test. The FWHM and the position of the line were fixed; only the abundance was varied. The noise was determined by the photon statistics. We also assumed that the continuum was 99% of our “best” choice and that Pd was the only contributor to the absorption at that wavelength. These choices gave a secure upper limit to the Pd abundance. Figure 2 gives an example of the  $5\sigma$  limit for BD -18 5550.

### 3.2. Sr Abundances

Another element useful for shedding light on early Galactic nucleosynthesis is Sr. Because it is made in the r, mains and weak s-processes, its ratio with other elements, such as Y, changes as contributions from various processes are made. Unfortunately, we found our synthesis of the strong resonance lines of SrII at 4077Å and 4215Å yielded different answers for the core and the wings of the lines. The

Sr II line is very deep in most of our stars, approaching depths of 20% of the continuum. The high layers of the atmospheric models probably have an incorrect temperature structure. Indeed, the Fe lines argue that such is the case (see Paper I) in these stars. So we decided to fit the wings of the lines using the linelists from Sneden et al. (1996) to determine the Sr abundance. In the solar system, there are four isotopes of Sr,  $^{84}\text{Sr}$ ,  $^{86}\text{Sr}$ ,  $^{87}\text{Sr}$ , and  $^{88}\text{Sr}$ , with  $^{88}\text{Sr}$  dominating the abundance in the solar system and  $^{84}\text{Sr}$  accounting for  $< 1\%$ . Only  $^{87}\text{Sr}$  has appreciable HFS. McWilliam et al. (1995) provide the wavelengths and gf-values for the 4215Å line; HFS constants are not available for the 4077Å line. The importance of HFS depends on the relative strength of the  $^{87}\text{Sr}$  contribution.  $^{88}\text{Sr}$  is the only Sr isotope produced in the r-process, so if the Sr in these stars is due only to the r-process (as we argue below) then no HFS needs to be considered. The main s-process produces mostly  $^{88}\text{Sr}$ , leaving another process, most likely the weak s-process to contribute substantial amounts of  $^{86}\text{Sr}$  and  $^{87}\text{Sr}$  (Arlandini et al. 1999). To test the effect of including the weak s-process isotopes in our synthesis, we subtracted Arlandini et al.’s main s-process yields from the total solar system abundances, which resulted in a Sr composition that was 35%  $^{86}\text{Sr}$ , 22%  $^{87}\text{Sr}$ , and 43%  $^{88}\text{Sr}$ . As suspected, using this combination of Sr isotopes decreased the derived Sr abundance from the 4215Å line by up to 0.3 dex. Because this affected all of our abundances in a similar fashion, the relative abundances change by a much smaller ( $< 0.1$  dex) amount. The wings of the lines are not a sensitive abundance indicator; we estimate observational errors of 0.15 dex for our abundances. Including the effect of uncertainties in model atmosphere parameters, in particular in the microturbulent velocity, raises the total error to 0.30 dex. Table 2 gives the Sr abundances derived assuming only  $^{88}\text{Sr}$  is present.

### 3.3. Other Abundances

We have already presented the abundances for other neutron-capture elements for the 22 stars in our sample in Paper I. Table 2 includes the  $[\text{Fe}/\text{H}]$  values derived in Paper I for all our stars, as well as abundances for Y, Zr and Ba, since those are the abundances most discussed in this paper. We have also plotted some abundance ratios from the literature. When error bars for these points are shown, they represent the addition in quadrature of the standard deviations of the mean for the two elements.

## 4. RESULTS

### 4.1. Overview

Figure 3 shows the abundances for three heavy-element-rich stars in our sample, as well as two extraordinary stars from the literature, CS 22892-052 (Sneden et al. 1996) and CS 31082-001 (Hill et al. 2002). The latter two are metal-poor ( $[\text{Fe}/\text{H}] \sim -3.0$ ) field giants as well, and show even larger enhancements of neutron-capture elements than any of the stars in our sample. This permitted the measurement of crucial elements such as U, Os, Ir, and Pb. The elements heavier than Ba and lighter than Yb show remarkable star-to-star consistency and very good agreement with the contributions of the r-process to the solar-system abundances ( $r_{ss}$ ). The recent work of Toenjes et al. (2001) and Hill et al. (2002) on CS 31082-001 has shown that the

TABLE 3  
ABUNDANCES

Star	[Fe/H]	Sr log $\epsilon$	$\sigma$	Y log $\epsilon$	$\sigma$	Zr log $\epsilon$	$\sigma$	Pd log $\epsilon$	$\sigma$	Ag log $\epsilon$	$\sigma$	Ba log $\epsilon$	$\sigma$
HD 29574	-1.85	1.24	0.30	0.27	0.16	1.07	0.16	...	...	...	...	0.54	0.26
HD 63791	-1.72	1.07	0.30	0.28	0.17	1.01	0.15	...	...	...	...	0.42	0.26
HD 88609	-2.96	-0.32	0.30	-0.80	0.09	0.02	0.09	< 0.07	...	...	...	-1.92	0.10
HD 108577	-2.36	0.35	0.30	-0.52	0.13	0.18	0.10	-0.69	0.25	-1.29	0.25	-0.35	0.21
HD 115444	-3.14	-0.51	0.30	-1.00	0.09	-0.30	0.08	< -0.49	...	...	...	-1.10	0.15
HD 122563	-2.75	-0.24	0.30	-0.80	0.10	-0.14	0.08	< -0.60	...	...	...	-1.80	0.11
HD 126587	-3.07	-0.28	0.30	-1.07	0.09	-0.36	0.08	< -0.53	...	...	...	-1.08	0.16
HD 128279	-2.38	0.06	0.30	-0.72	0.15	-0.09	0.14	< -0.27	...	...	...	-0.74	0.17
HD 165195	-2.31	0.68	0.30	-0.38	0.08	0.46	0.11	...	...	...	...	-0.43	0.20
HD 186478	-2.60	0.49	0.30	-0.48	0.12	0.29	0.06	-0.67	0.25	-1.32	0.25	-0.55	0.22
HD 216143	-2.22	0.87	0.30	-0.16	0.14	0.53	0.10	...	...	...	...	-0.30	0.23
HD 218857	-2.18	0.61	0.30	-0.43	0.13	...	...	...	...	...	...	-0.47	0.24
BD -18 5550	-3.04	-1.20	0.30	-1.81	0.05	-1.22	0.09	< -0.55	...	...	...	-1.67	0.16
BD -17 6036	-2.76	-0.40	0.30	-1.15	0.11	-0.48	0.09	< -0.10	...	...	...	-1.09	0.18
BD -11 145	-2.48	0.31	0.30	-0.57	0.11	0.09	0.14	...	...	...	...	-0.29	0.23
BD +4 2621	-2.51	0.18	0.30	-0.69	0.14	0.03	0.08	< -0.41	...	...	...	-1.21	0.23
BD +5 3098	-2.73	0.11	0.30	-0.87	0.13	-0.14	0.14	< 0.41	...	...	...	-0.96	0.18
BD +8 2548	-2.11	0.78	0.30	-0.15	0.15	0.57	0.09	-0.36	0.25	-0.78	0.25	-0.07	0.24
BD +9 3223	-2.28	0.71	0.30	-0.23	0.14	0.44	0.17	...	...	...	...	-0.13	0.19
BD +10 2495	-2.07	0.77	0.30	-0.16	0.14	0.48	0.17	...	...	...	...	0.03	0.24
BD +17 3248	-2.10	0.94	0.30	0.10	0.16	0.75	0.18	...	...	...	...	0.51	0.14
BD +18 2890	-1.73	1.21	0.30	0.38	0.16	1.03	0.14	...	...	...	...	0.63	0.29

good agreement does not extend beyond Yb to Th and U. Our new Pd and Ag values show a stronger odd-even effect than  $r_{ss}$ , as seen by Sneden et al. (2000a) in CS 22892-052. The additional abundances measured in CS 22892-052 show that this odd-even pattern extends from Nb to Cd. The lightest neutron-capture elements we have measured, Sr, Y, and Zr, also show a similar pattern from star-to-star, although even with the small number of stars in Figure 3 the dispersion in the light-to-heavy neutron-capture element ratios, such as Y/Ba, is obvious. There is a lack of dispersion in the ratios between the intermediate elements, such as Pd and the heavy elements.

#### 4.2. Ba through Yb

From a quantitative standpoint, Johnson & Bolte (2001) showed that the abundances of Ba through Yb in all stars agree well with  $r_{ss}$  and that the scatter is consistent with observational error. Previous work on field stars with  $[\text{Fe}/\text{H}] < -2.0$  has given a similar result (e.g. Gilroy et al. 1988; Sneden et al. 1996; McWilliam 1998). Sneden et al. (2000b) analyzed the abundances of Ba, La, Ce, Nd, Sm, Eu, Gd and Dy in three red giants from the metal-poor globular cluster M 15, and found the  $r_{ss}$  pattern in each of these stars as well.

#### 4.3. Sr, Y, and Zr

We also find that within the narrow mass range spanned by Sr, Y and Zr ( $A=84 - 96$ ), the abundance pattern repeats itself from star-to-star. In Figure 4a, we have plotted  $[\text{Y}/\text{Zr}]$  vs.  $[\text{Fe}/\text{H}]$  and find that all the scatter in the plot (aside from the M15 stars) is due to observational error. A similar result for field dwarfs with  $[\text{Fe}/\text{H}] < -1.5$  was found by Zhao & Magain (1991). We have included the three red giants from M 15 (Sneden et al. 2000b) in Figure 4a. The M 15 stars have similar  $[\text{Y}/\text{Zr}]$  values, but on average they are lower than the field stars' values. The

M 15  $[\text{Y}/\text{Zr}]$  values are based on at least three lines of each element, and the same source, but not exactly the same lines, was used for the gf-values. So it seems unlikely that observational error could provide the entire explanation. However, observations of stars in more globular clusters, particularly at the high S/N necessary to measure the

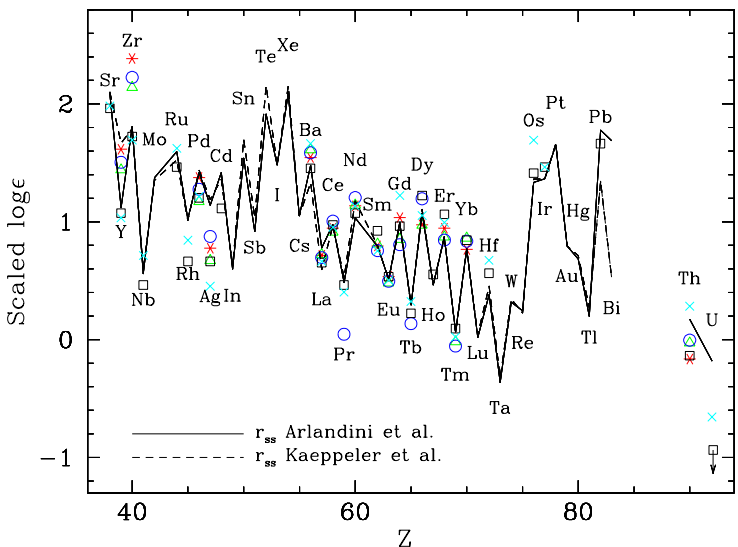


FIG. 3.— Abundances from Sr to Yb for HD 108577 ( $\Delta$ ), HD 186478 ( $*$ ) and BD +8 2548 ( $\circ$ ) from this work. We have also plotted the abundances for CS 22892-052 (Sneden et al. 2000a) (open squares) and CS 31082-001 (Hill et al. 2002) ( $\times$ ). These abundances have been scaled up to the Arlandini et al. (1999)  $r_{ss}$  using the Ba, La, Ce, Sm and Eu abundances. To show the uncertainties in  $r_{ss}$ , we have included the  $r_{ss}$  from Käppeler et al. (1989).

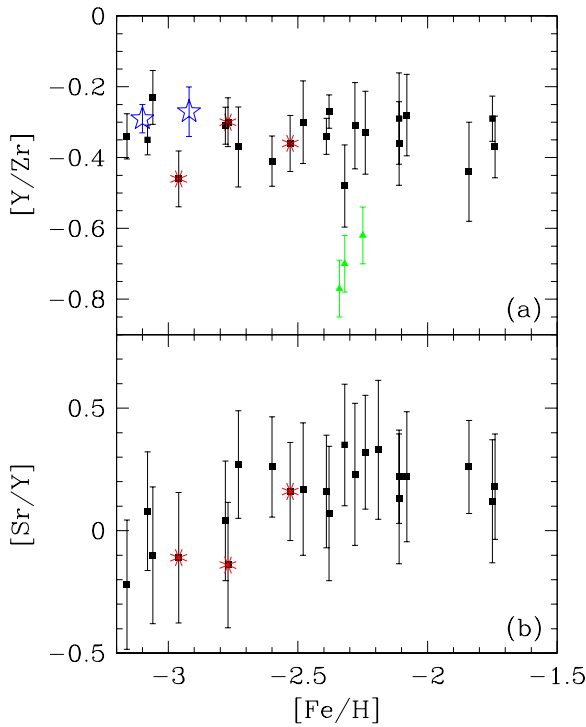


FIG. 4.— (a)  $[Y/Zr]$  vs.  $[Fe/H]$  for stars in our sample (squares) as well as CS 22892-052 and CS 31082-001 (stars) and M 15 giants (triangles). Asterisks mark the three stars in our sample with  $[Y/Ba] > 0.4$  dex. While there is good agreement among the  $[Y/Zr]$  values for the field stars, the M 15 data are systematically lower. (b)  $[Sr/Y]$  vs.  $[Fe/H]$  for stars in our sample. Since our Sr values were determined using the wings of the lines, instead of the EW, we have not included CS 22892-052 or CS 31082-001 in this plot. The lower values at lower metallicities are due to difficulties of deriving abundances from the wings of the lines. The observational errors are enough to explain all the scatter.

Zr II lines accurately, would be helpful. The  $[Sr/Y]$  values shown in Figure 4b also are consistent with one  $[Sr/Y]$ , especially since the  $\sim 0.3$  dex difference between the lowest metallicity stars and the rest of the sample is likely due to the difficulties of determining abundances from the wings of lines of varying strength. The plot looks substantially the same if we use the abundances from the  $4215\text{\AA}$  line with HFS and the isotope percentages given in §3.2.

There is certainly scatter in the light-to-heavy neutron-capture element ratios greater than can be explained by observational error. Figure 5 shows the  $[Y/Ba]$  ratio for our sample as well as for data from McWilliam et al. (1995), McWilliam (1998) and Fulbright (2000) taken from the literature. The literature studies were drawn from recent papers that had data with high-resolution and large wavelength coverage of metal-poor stars. Our results (Figure 5) confirm the large scatter seen previously in the ratio of light-to-heavy neutron capture elements (e.g. McWilliam et al. 1995; Ryan et al. 1996; Westin et al. 2000) While we have chosen to plot  $[Y/Ba]$  because their lines are prominent in all of our spectra, we note that using Sr or Zr in place of Y, or any element from La to Yb in place of Ba would have resulted in a similar plot, since the abundance ratios within each group are constant.

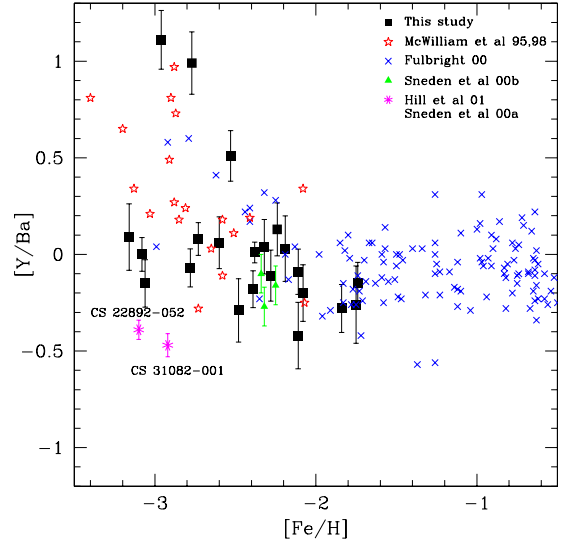


FIG. 5.—  $[Y/Ba]$  for the stars from this study as well as from the literature. There is a 1.5 dex scatter in  $[Y/Ba]$  which decreases as metallicity increase. The two stars with extreme overabundances of the heavy r-process elements, CS 22892-052 and CS 31082-001 mark the lower limit of observed  $[Y/Ba]$  values. The M 15 stars, with their very small dispersion in  $[Y/Ba]$ , are marked by solid triangles.

#### 4.4. *Pd and Ag*

Does a similar scatter exist in the  $[Pd/Y]$  or  $[Pd/Ba]$  values? For the three stars in our sample with measurements, the  $[Pd/Y]$  and  $[Pd/Ba]$  values are consistent with a single value. The  $5\sigma$  upper limits quoted for Pd cannot rule out that all stars have the ratio for these elements. Higher S/N data, especially of stars with high  $[Y/Ba]$  ratios such as HD 88609 and HD 122563, would answer this question. We find a similar  $[Pd/Ag]$  ratio to the values for CS22892-052 (Sneden et al. 2000a) and CS 31082-001 (Hill et al. 2002) in the three stars in our sample with measurements. It is important to keep in mind that this sample is biased to stars with large  $[\text{heavy-neutron-capture}/\text{Fe}]$  ratios and may not be representative of all stars. However, the consistent  $[Pd/Ag]$  ratio we are finding may indicate one r-process pattern in the intermediate mass elements in metal-poor stars.

#### 4.5. *Summary*

Our observational results can be summarized as follows: There is good agreement between Ba and Yb with  $r_{ss}$  for all the stars, both field and cluster, in our sample. For the small number of stars with Pd and Ag measurements, we find indications of an increased odd-even effect for Pd and Ag compared to  $r_{ss}$ . There is a large spread in  $[Y/Ba]$ , but all the field stars have similar values for  $[Y/Zr]$  and  $[Sr/Y]$ . However, the  $[Y/Zr]$  values for stars in M 15 are  $\sim 0.3$  dex lower.

### 5. DISCUSSION

#### 5.1. *Origin of the neutron-capture elements in metal-poor stars*

##### 5.1.1. *Uncertainties in theoretical r-process abundances*

Ideally, the abundance ratios produced by the r-process would be known accurately from theory, and the results from metal-poor stars could be interpreted in light of that information. But because of the unknown physical properties of the progenitor nuclei near the neutron-drip line and the unknown physical conditions during the r-process, the most useful predictions actually rely on s-process calculations. These s-process models are fit to the s-only nuclei and then subtracted from the total isotopic abundances present in the solar system. Therefore, depending on the results of the s-process model,  $r_{ss}$  can change. This change can be substantial for elements that in the solar system are mostly produced by the s-process, such as Sr, Y, and Zr, where changes of 10% in the s-process predictions can lead to changes of over 100% in  $r_{ss}$ . We have illustrated the consequences in Figure 3. Here we have plotted  $r_{ss} = \log \epsilon_{tot} - \log \epsilon_{mains-process}$  from two literature sources: Käppeler et al. (1989) and Arlandini et al. (1999). The main difference between the two studies lies in the physical conditions during the neutron-captures onto the seed nuclei. Käppeler et al. used the “classical” model, where the neutron exposure is assumed to have an exponential distribution and the temperature does not depend on time. Arlandini et al. instead use the physical conditions predicted by AGB models, where neither assumption holds. This substantially modifies the abundances, particularly of Y. Figure 3 shows that if the Arlandini results, instead of the Käppeler results, are used, there is no conflict between  $r_{ss}$  and the abundances of CS 22892-052 in the Sr, Y and Zr region. This does not mean that the problem of the abundance ratios of the lighter neutron-capture elements has been solved, but rather that uncertainties in  $r_{ss}$  remain at a large enough level to confuse our interpretations of the abundances in metal-poor stars.

### 5.1.2. Theoretical predictions for the r-process

Theoretical results show that the r-process alone is responsible for the production of the elements heavier than Zr in the early Galaxy. The main s-process is not efficient at low metallicities (Gallino et al. 1998). Combined with the lifetimes of the progenitor low-mass AGB stars, this leads to an 0.7 Gyr time lag to the appearance of s-process nucleosynthesis in the early Galaxy (Raiteri et al. 1999). No other process contributes significant amounts of the heavier nuclei. The main s-process can never build the heaviest nuclei, such as Th and U (Clayton & Rassbach 1967) so these must be r-only nuclei at all times. Kratz et al. (2000) found that requiring a high minimum neutron density during the r-process could duplicate the enhanced odd-even staggering in the Pd-Ag region and still match the pattern seen in the heavier elements. Sr, Y and Zr are produced in the r-process and are also seeds for the creation of the heavier elements such as Pd, Ba, Yb, etc. In fact, if the neutron density is high enough, it is possible for so many neutrons to be captured that little Sr, Y, and Zr is produced. (Kratz et al. 2000; Pfeiffer, Ott & Kratz 2000). Depending on the physical conditions in the r-process event, very different [Y/Ba] ratios, for example, can be created. Thus, it is possible for the r-process to explain all the features we observe.

### 5.1.3. Theoretical predictions for the weak s-process

However, the r-process may not be the only contributor to the light neutron-capture elements. The weak s-process, which occurs in short-lived, massive stars, is another possible source for Sr, Y, Zr in low-metallicity stars. As mentioned earlier, the conditions in massive stars do not lead to the production of heavier nuclei than A~90, so contributions from the weak s-process are not expected for elements heavier than Zr. Prantzos et al. (1990) argued that the weak s-process should be extremely inefficient at  $[\text{Fe}/\text{H}] \sim -3.0$  because of the lack of seed nuclei and the presence of primary neutron poisons. However, there are several uncertain quantities in those calculations, particularly crucial neutron capture cross-sections, which could alter the efficiency of the weak s-process in metal-poor stars by factors of  $\sim 5$  (Prantzos et al. 1990; Rayet & Hashimoto 2000), so contributions to Sr, Y, and Zr from the weak s-process cannot be dismissed.

#### 5.1.4. Constraints from observations: the r-process

The observed good agreement between the heavier elements (Ba-Yb) and  $r_{ss}$  is empirical evidence for the predominance of the r-process in the early Galaxy. Adding contributions from the main s-process to  $r_{ss}$  results in a poor fit with the abundances in metal-poor stars (Gilroy et al. 1988; Sneden et al. 1996; Johnson & Bolte 2001) Goriely & Arnould (1997) showed that the pattern from Ba to Yb is not very sensitive to the exact conditions of temperature, entropy, etc. in which the r-process takes place, so this abundance pattern is perhaps a robust sign of the r-process.

Observations also show that the r-process contributes at least some fraction to the lighter neutron-capture elements. First, we note that the values for [Y/Zr] and [Sr/Y] that we find are close to the those we would predict if we assumed that all possible r-process isotopes were produced in equal amounts as discussed by Goriely & Arnould. Y has one stable r-process isotope, Zr has five, and Sr has one. This leads to  $[\text{Y/Zr}] = -0.34$  and  $[\text{Sr/Y}] = 0$ , similar to what is seen in Figure 4.

Then there are the cases of CS 22892-052 and CS 31082-001. These two stars show large enhancements of the heavy neutron-capture elements, such as Ba, which are due to the r-process (Sneden et al. 1996). They also are enriched in Sr, Y and Zr to a similar degree. It is more likely that both the Ba and the Y were created in the same r-process event than that these two stars were enriched by an r-process event that created Ba, but not Y, and were also enriched in Y by a separate, weak s-process event. (McWilliam 1998). Even better evidence comes from M15. Like most other Galactic globular clusters, stars in M 15 are homogeneous in their chemical composition when considering the  $\alpha$ - and iron-peak elements, with the exception of elements that have been affected by mixing (Sneden et al. 1997). However, the [Ba/Fe] values showed a spread of 0.8 dex. Examination of other heavy neutron-capture elements, such as Eu, showed that the heavy neutron-capture elements in all the stars was due to the r-process (Sneden et al. 2000b). Somehow, the r-process ejecta had managed to spread itself very unevenly in this cluster. In Figure 5, we have included the [Y/Ba] from the three stars of Sneden et al. (2000b). The values for these stars are indistinguishable given the observational errors. It is unreasonable to expect an independent

process to have dispersed its ejecta in exactly the same pattern as the r-process event. So the Y in CS 22892-052, CS 31082-001 and M15 comes from the r-process.

### 5.1.5. Constraints from observations: the weak s-process

We can then use the knowledge that the Y in these stars was produced in the r-process in the early Galaxy, to evaluate the possible contributions of other processes to the lighter neutron capture elements. The [Y/Zr] ratio is sensitive to contributions from different processes. In Figure 4, we saw that stars have the same [Y/Zr] regardless of their [Y/Ba] value; the three stars from our sample that had high [Y/Ba] values in Figure 5 are hidden amidst the rest of the sample. Because the [Y/Zr] ratio is very sensitive to the production method, as we discuss in detail below, the constant [Y/Zr] values make it very difficult to attribute the high [Y/Ba] values observed to the addition of light elements from another process that was not the r-process.

Let us take the case of CS 22892-052 ( $[Y/Ba] = -0.39$ ) and HD 122563 ( $[Y/Ba] = 0.99$ ). If we first assume that CS 22892-052's  $[Y/Ba]$  represents the minimum production in an r-process event, we then find that 96% of the Y in HD 122563 must have been produced in another process. The weak s-process yields of Raiteri et al. (1993) predict a [Y/Zr] value for HD 122563 of 0.25, some 0.55 dex larger than measured. The situation is not significantly altered by having some of the Y in both stars from the weak s-process. It is very difficult to hide even a small contribution from the weak s-process when [Y/Zr] is constant. This is because with a predicted production [Y/Zr] production ratio of 0.43 dex, the weak s-process is very different from the [Y/Zr] expected from the r-process ( $-0.33$  according to Arlandini et al. (1999)). It is unclear whether the predictions of Raiteri et al. are valid at all points in Galactic history. In order to understand our observational results, it is crucial to know the expected range of [Y/Zr] values for other processes that could contribute to the the heavy elements in the early Galaxy. If there are other processes, their [Y/Zr] production ratio must be similar to that of the r-process. The simplest solution, however, is to have the production of all neutron-capture elements in the r-process only in the early Galaxy.

### 5.2. The r-process in the early Galaxy

Although at present we favor a picture where all the neutron-capture elements in metal-poor stars were created in the r-process, the spread in [Y/Ba] shows that there is not one universal r-process pattern. The abundances in CS22892-052 and CS31082-001 have already shown that (Sneden et al. 2000a; Hill et al. 2002). In addition, Wasserburg et al. (1996) found evidence in the abundances of extinct radioactive nucleotides in the solar system that some r-process events produce much larger  $^{129}\text{I}/^{182}\text{Hf}$  ratios than others. Because of the scatter in [Y/Ba], the abundances in metal-poor stars give support for some r-process events producing mostly the lighter neutron-capture elements, while other events favor the production of Ba and heavier. Some events also appear to manufacture more of the heaviest elements such as Th and U. Such an event must have polluted CS 31082-001. Whether one phenomenon, such as the neutrino-wind in Type II SN, can provide a wide enough range of conditions to account

for the diversity seen, or whether a variety of phenomena, from neutron-star mergers to He-burning regions, are needed is not yet clear.

## 6. CONCLUSION

Abundance ratios of neutron-capture elements in metal-poor stars show both striking similarities and large dispersions. There is real scatter in the [Y/Ba] ratios observed and differences between metal-poor stars and  $r_{ss}$  in the [Pd/Ag] ratio. The Sr-Y-Zr and the Ba-Yb regions show similar abundance patterns in all stars in the Paper I sample, with some deviation in the lighter elements in the red giants from M 15. The M 15 giants provide the strongest evidence that the light neutron-capture elements in metal-poor stars can be produced in the same events as the heavy neutron-capture elements, since stars with very different [Ba/Fe] have identical [Y/Ba]. Similar evidence is provided by CS 22892-052 and CS 31082-001, which have large enhancements in both Y and Ba.

Theoretical results show that the main s-process cannot produce substantial amounts of the neutron-capture elements in low metallicity stars. This result is supported by the good agreement between abundance pattern in the Ba region in our sample of stars and  $r_{ss}$ . The weak s-process potentially could contribute to elements with  $A < 90$ . However, the constant abundance ratios of [Sr/Y] and [Y/Zr] precludes substantial contributions from processes other than the r-process in the early Galaxy. As a result, the abundances of the neutron-capture elements in metal-poor stars provide strong constraints on the r-process. Any model of the r-process must explain the scatter seen in [Y/Ba] and [Ba/Th]. In addition, the models need to reproduce the enhanced odd-even effect in the Pd-Ag region. The variety of phenomena proposed for the r-process shows that the r-process production need not be confined to one kind of event, which could aid in describing the dispersion seen.

Some of the data presented herein were obtained at the W.M. Keck Observatory, which is operated as a scientific partnership among the California Institute of Technology, the University of California and the National Aeronautics and Space Administration. The Observatory was made possible by the generous financial support of the W.M. Keck Foundation. We would like to thank Andy McWilliam for a careful reading of a draft of this paper and Chris Sneden for generously making software and linelists available. This work was supported by NSF AST-0098617.

## REFERENCES

Anders, E. & Grevesse, N. 1989, *Geo. Cos. Acta*, 53, 503 rawford, J.

Arlandini, C. Käppeler, F., Wissak, K., Gallino, R., Lugaro, M., Busso, M., & Straniero, O. 1999, *ApJ*, 525, 886

Biemont, E., Grevesse, N., Kwiatkowski, M., & Zimmermann, P. 1982, *A&A*, 108, 127

Burbidge, E. M., Burbidge, G. R., Fowler, W. A., & Hoyle, F. 1957, *Rev. Mod. Phys.*, 29, 547

Burris, D. L., Pilachowski, C. A., Armandroff, T. E., Sneden, C., Cowan, J. J., & Roe, H. 2000, *ApJ*, 544, 302

Cameron, A. G. W. 1957, *PASP*, 69, 201

Clayton, D. D. & Rassbach, M. E. 1967, *ApJ*, 148, 69

Couch, R. G., Schmiedekamp, A. B., & Arnett, W. D. 1974, *ApJ*, 190, 95

Cowan, J. J., Cameron, A. G. W., & Truran, J. W. 1985, *ApJ*, 294, 656

Crawford, J. L., Sneden, C., King, J. R., Boesgaard, A. M., & Deliyannis, C. P. 1998, *AJ*, 116, 2489

Freiburghaus, C., Rembges, J.-F., Rauscher, T., Kolbe, E., Thielemann, F.-K., Kratz, K.-L., Pfeiffer, B., & Cowan, J. J. 1999, *ApJ*, 516, 381

Freiburghaus, C., Rosswog, S., & Thielemann, F.-K. 1999, *ApJ*, 525, L121

Fuhr, J. R. & Wiese, W. L. 1996, in *CRC Handbook of Chemistry and Physics*, ed. D. R. Lide (Boca Raton, FL: CRC Press), 10-128

Fulbright, J. 2000, *AJ*, 120, 1841

Gallino, R., Arlandini, C., Busso, M., Lugaro, M., Travaglio, C., Straniero, O., Chieffi, A., & Limongi, M. 1998, *ApJ*, 497, 388

Gilroy, K. K., Sneden, C., Pilachowski, C., & Cowan, J. J. 1988, *ApJ*, 327, 298

Goriely, S. & Arnould, M. 1997, *A&A*, 322, L29

Hill, V., et al. 2002, *A&A*, 387, 560

Johnson, J. A.., 2002, *ApJS*, 139, 219

Johnson, J. A. & Bolte, M. 2001, *ApJ*, 554, 888

Käppeler, F., Beer, H., & Wissak, K. 1989, *Rep. Prog. Physics*, 52, 945

Kratz, K.-L., Pfeiffer, B., Thielemann, F.-K., & Walters, W. B. 2000, *Hyperfine Interactions*, 129, 185 (astro-ph/9907071)

Kurucz, R. L. & Bell, B. 1995, 1995 *Atomic Line Data*, CD-ROM 23, Cambridge, MA: Smithsonian Astrophysical Observatory.

Lattimer, J. M. & Schramm, D. N. 1974, *ApJ*, 192, L145

McWilliam, A. 1998, *AJ*, 115, 1640

McWilliam, A., Preston, G. W., Sneden, C. & Searle, L. 1995, *AJ*, 109, 2757

O'Brian, T. R., Wickliffe, M. E., Lawler, J. E., Whaling, W., & Brault, J. W. 1991, *J. Opt. Soc. Am. B*, 8, 1185

Otsuki, K., Tagoshi, H., Kajino, T., & Wanajo, S. 2000, *ApJ*, 533, 424

Pfeiffer, B., Ott, U., & Kratz, K.-L. 2001, *Nuc. Phy. A*, 688, 465

Pickering, J. C. 1996, *ApJS*, 107, 811

Prantzos, N., Hashimoto, M., & Nomoto, K. 1990, *A&A*, 234, 211

Qian, Y.-Z. & Woosley, S. E. 1996, *ApJ*, 471, 331

Raiteri, C. M., Gallino, R., Busso, M., Neuberger, D., & Käppeler, F. 1993, *ApJ*, 419, 207

Raiteri, C. M., Villata, M., Gallino, R., Busso, M., & Cravanzola, A. 1999, *ApJ*, 518, L91

Rayet, M. & Hashimoto, M. 2000, *A&A*, 354, 740

Ross, J. E. & Aller, L. H. 1972, *Sol. Phy.*, 25, 30

Rosswog, S., Davies, M. B., Thielemann, F.-K., & Piran, T. 2000, *A&A*, 360, 171

Ryan, S. G., Norris, J. E., & Beers, T. C. 1996, *ApJ*, 471, 254

Sneden, C., Cowan, J. J., Ivans, I. I., Fuller, G. M., Burles, C., Beers, T. C., & Lawler, J. E. 2000a, *ApJ*, 533, L139

Sneden, C., Kraft, R. P., Shetrone, M. D., Smith, G. H., Langer, G. E., & Prosser, C. F. 1997, *AJ*, 114, 1964

Sneden, C., Johnson, J., Kraft, R. P., Smith, G. H., Cowan, J. J., & Bolte, M. S. 2000b, *ApJ*, 536, L85

Sneden, C., McWilliam, A., Preston, G. W., Cowan, J. J., Burris, D. L., & Armosky, B. J. 1996, *ApJ*, 467, 819

Takahashi, K., Witt, J., & Janka, H.-Th. 1994, *A&A*, 286, 857

Toenjes, R., Schatz, H., Kratz, K.-L., Pfeiffer, B., Beers, T. C., Cowan, J. & Hill, V. 2001, in *Astrophysical Ages and Timescales*, ASP Conf. Series Vol 245, Ed T. von Hippel, C. Simpson and N. Manset San Francisco, ASP, p. 376 astroph/010433

Truran, J. W., 1981, *A&A*, 97, 391

Truran, J. W., Cowan, J. J., & Fields, B. D. 2001, *Nuc. Phy. A*, 688, 330

Vogt, S. S., 1987, *PASP*, 99, 1214

Vogt, S. S., et al., 1994, *SPIE*, 2198, 362

Wanajo, S., Kajino, T., Mathews, G. J., & Otsuki, K. 2001, *ApJ*, 554, 578

Wasserburg, G. J., Busso, M., & Gallino, R. 1996, *ApJ*, 466, L109

Westin, J., Sneden, C., Gustafsson, B., & Cowan, J. J. *ApJ*, 530, 783

Witti, J., Janka, H.-Th., & Takahashi, K. 1994, *A&A*, 286, 841

Woosley, S. E. & Hoffman, R. D. 1992, *ApJ*, 395, 202

Woosley, S. E., Wilson, J. R., Mathews, G. J., Hoffman, R. D., & Meyer, B. S. 1994, *ApJ*, 433, 229

Zhao, G. & Magain, P. 1991, *A&A*, 244, 425